Technical Progress Report

MECHANISMS OF MONSOON RAINFALL IN THE INDO-PACIFIC REGION

David W. Martin
Principal Investigator

Barry B. Hinton
Co-Investigator

for the period
1 June 1994--30 November 1994

University of Wisconsin-Madison

Space Science & Engineering Center
1225 West Dayton Street
Madison, WI 53706

Grant NAGW-3641

Through the Nimbus 7 Scanning Multichannel Microwave Radiometer we shall map eight years of rainfall over the tropical western Pacific and Indian Oceans. Our maps will document trends over the period and also cycles on the scale of the Madden-Julian oscillation, the monsoon and El Niño-Southern Oscillation. To construct them we will apply a generalized version of our Indian Ocean SMMR algorithm to the JPL record of SMMR radiances.

Considering acquisiton cost, data quality and archive medium, we decided last spring in favor of the SMMR record of the Jet Propulsion Laboratory over that of the National Space Science Data Center. This autumn's review of the reprocessing effort raised only one concern about that decision, delay in acquiring the data. On the other hand, it suggested a benefit, uniform grid of radiances. This uniform grid may enable us to skip the remapping step in our procedure. We expect to receive the first year of reprocessed data early in January.

Dr. S. V. Singh has sent us monthly rainfall for subdivisions of India for a period which includes the SMMR record. We are assembling files containing monthly maps of *SST*, *W*, *RH*, and Z_{fr}. The last two items have to be inferred from scattered studies in the literature (*e.g.* of latitude distributions of $T_{air}(Z)$ along restricted longitude sections). *SST*, and *W*, are more conveniently available in the COADS data base.

In the retrieval algorithm, rain rate implied by an individual SMMR channel R_i is considered to be a function of the channel's brightness temperature T_B and several environmental parameters which vary with location and time. The environmental parameters are sea surface temperature (*SST*), relative humidity (*RH*), wind speed (*W*) and freezing level (Z_{fr}). Air temperature (which is relatively unimportant) has been assumed to be equal to SST temperature at the surface, and to decrease upward at a climatological lapse rate.

A fraction of the area of each field of view of SMMR is covered by rain, the balance is not. For a model of the rain no-rain partition we have used results of Graves. (See upper panel of Plate 1.) In the figure his results have been fitted to curves of the form $[a - b \cdot exp(-R/c)]$. R_i and the other quantities are all interpreted as averages over a channel's field of view —a very good approximation for the environmental variables, but not for rain rate itself. The *R* quantities are modeled as field-of-view means over *distributions* of local rain rates which have significant variability on scales much less than the dimensions of a field of view.

The rain rate over the raining fraction is described by a gamma distribution. The lower panel of Plate 1 illustrates the nature of this distribution for various values of the mean rain rate. At extremely low mean rates the limiting shape is exponential. At very high mean rain rates it is log-normal.

The main variation of R_i is with T_B. Other effects are treated as perturbations. Consequently, $R_i(T_B, SST, RH, W, Z_{fr})$ is well approximated by an expression of the form,

$$R_i = R_{0i} + \frac{\partial R_i}{\partial (RH)}(RH - 80) + \frac{\partial R_i}{\partial (SST)}(SST - 27.5) + \frac{\partial R_i}{\partial (W)}(W - 7) + \frac{1}{2}\frac{\partial^2 R_i}{\partial (W)^2}(W - 7)^2 + \frac{\partial R_i}{\partial (Z_{fr})}(Z_{fr} - 4.5) \quad (1)$$

in which the subscript "i" designates the channel, and the subscript "0" designates the rain rate as a function of the ith channel brightness temperature, T_{Bi}, for a set of nominal environmental conditions: 80% relative humidity, 27.5 °C sea surface temperature, 7 m s^{-1} wind speed, and a freezing level at 4.5 km. The form of (1) is suggested by the Taylor series expansion of an arbitrary continuous function. Note, however, that two terms have been retained for the wind variation. The partial derivatives in (1) are all obtained from a radiative transfer model for this set of reference conditions.

Arbitrarily we have elected to replace channel 10 by an 11th synthetic channel ($T_{B\,V37} - T_{B\,H37}$). This does not change the information content of the total set of channels, but follows previous precedent. In addition, we do not intend to use the two lowest frequency channels (6.6 GHz) because of their poor spatial resolution. Thus, we will actually use eight of 11 indexed channels ($i = 1, \ldots, 11$) to form a multichannel rain estimate. For generality, the unused channels may still appear in equations or sums, but will be associated with a weight of zero.

Note that the curves in Plate 2, which illustrate $R_{0i}(T_{Bi})$ [the leading term in (1)], are double valued for frequencies above 10.7 GHz. In the figure they are represented by pairs of curves crossing at a common point. At this common point scattering by precipitating ice particles (which tends to decrease T_{Bi}) begins to dominate over emission by precipitating liquid drops (which tends to increase T_{Bi}). In practice, because of the distribution of rain rates in nature, area mean rain rates will almost always lie on the lower of the two branches of these curves —except for the 37 GHz channels. In any case, the ambiguity in other channels can be resolved with the help of the 10.7 GHz channels if we assume these are never far beyond their crossing points ($R > 50$ mm/h).

The partial derivatives in (1) are illustrated in the panels of Plate 3 for the eight useful channels. Note that dashed portions of the curves represent negative values. Like $R_{0i}(T_{Bi})$ these curves are typically double valued. When viewed as functions of T_{bi}.the curves turn back at the T_B value corresponding to the R_0 crossover point. Because $\partial R_{0i}(T_{Bi})/\partial T_{Bi} \rightarrow 0$ where the two branches of the $R_{0i}(T_{Bi})$ function join, there are associated divergences ($\rightarrow \pm\infty$) in the other partial derivatives.

Once the individual channel rain estimates are obtained, they are combined using a set of weights chosen optimally to minimize the expected multi-channel error. In the least square sense this optimization is achieved when the error variance[1] contributed by each channel is equal to the error variance contributed by any other channel. Assuming our estimates of the environmental parameters are unbiased, and that our radiative transfer model is unbiased, the error of an individual channel, R_i, is given by (2), in which the δ quantities are the root mean square errors of the environmental parameters. Of course these errors can never be known exactly, so in practice we must estimate them. We have tentatively assumed the following δ values: 3°C for SST, 5% for RH, 0.5 km for the freezing level and 3 m s^{-1} for wind.

[1] "Error variance" refers to the squared difference of the true and model-calculated values.

$$(\delta R_i)_{environmental} = \left\{ \left(\frac{\partial R_i}{\partial (RH)} \delta_{RH} \right)^2 + \left(\frac{\partial R_i}{\partial (SST)} \delta_{SST} \right)^2 + \left(\frac{\partial R_i}{\partial (W)} \delta_W + \frac{1}{2} \frac{\partial^2 R_i}{\partial (W)^2} 2(W-7)\delta_W \right)^2 + \left(\frac{\partial R_i}{\partial (Z_{fr})} \delta_{Z_{fr}} \right)^2 \right\}^{1/2} \quad (2)$$

In addition, there is an error in each R_i due to measurement errors in T_{Bi}, that is, "noise." The magnitude of δT_{Bi} is thought to be about 2° for all ten original SMMR channels. It follows that δT_{Bi} for channel 11, the synthetic *V37-H37* channel, would be

$$\delta T_{B11} = \sqrt{\left(\delta T_{B9}\right)^2 + \left(\delta T_{B10}\right)^2} = \sqrt{2} \cdot \delta T_{Bi} \quad \text{for } i = 1, \cdots, 10 \quad (3)$$

The expression for the rain error due to channel noise of brightness temperature is given in (4).

$$\delta R_{i\,noise} = \left| \frac{\partial R}{\partial T_{Bi}} \right| \cdot \delta T_{Bi} \quad (4)$$

The $\partial R_i / \partial T_{Bi}$ illustrated in Plate 3. It follows that the total error variance is given by (5)

$$(\delta R_i)^2_{total} = \left\{ \left(\frac{\partial R_i}{\partial (RH)} \delta_{RH} \right)^2 + \left(\frac{\partial R_i}{\partial (SST)} \delta_{SST} \right)^2 + \left(\frac{\partial R_i}{\partial (W)} \delta_W + \frac{1}{2} \frac{\partial^2 R_i}{\partial (W)^2} 2(W-7)\delta_W \right)^2 + \left(\frac{\partial R_i}{\partial (Z_{fr})} \delta_{Z_{fr}} \right)^2 + \left(\frac{\partial R_i}{\partial T_{Bi}} \delta T_{Bi} \right)^2 \right\} \quad (5)$$

The weights, w_i, needed for the composite rain estimate are

$$w_i = \begin{cases} \dfrac{(\delta R_i)^2_{total}}{\sum_{j=1}^{11} (\delta R_j)^2_{total}} & \text{Over the oceans, far from land} \\ 0 & \text{Near land, or channels 1, 2, or 10} \end{cases} \quad (6)$$

Our optimized estimate of rain rate is thus given by (7).

$$R = \sum_{i=1}^{11} (w_i \cdot R_i) \tag{7}$$

As discussed above, $w_i \equiv 0$ for $i = 1$, 2, and 10. One set of weights for nominal conditions is illustrated in the larger panel of Plate 4. These could be independently calculated for each field of view processed if there were variations in the δ values of environmental parameters with time and location. Closer inspection of (5) and (6) shows, however, that for w_i the absolute magnitudes of the δ's are not important —it is their size *relative to each other* that matters. The effects of varying the δ's one at a time, are illustrated in the smaller panels of Plate 4. While some adjustments are evident, these illustrations suggest that a formulation in which the weights are made functions of the rain rate only (by assigning constant standard values to the environmental δ's) could be used for the sake of computational simplicity.

Except for these modifications, we have installed the algorithm on a UNIX workstation. Because it serves as a processor rather than an ingestor, the workstation should convert radiances into rainrates more cheaply than the mainframe.

Over the next month we will digitize the monthly subdivision rainfall and install the modifications to the UNIX version of the algorithm. After satisfying ourselves that the UNIX algorithm works, we will remove the mainframe version of the algorithm. We will cross-check the first set of JPL SMMR data against NSSDC data. If the JPL data prove to be reliable, we will test the UNIX algorithm. If the algorithm passes this test, we will calculate and map rainfall for the first three years of the record. If the new maps pass checks against the old, we will complete the mapping. Finally, we will begin to merge the subdivision and SMMR records.

Support for the Principal Investigator is as follows.

TITLE	AGENCY	AMOUNT	PERIOD	PERCENT OF EFFORT
Mechanisms of Monsoon Rainfall in the Indo-Pacific Region	NASA	$186, 000	1 Jun 1993- 31 May 1995	25
A Tropical Rainfall Analysis Experiment for TRMM Using Ancillary Satellite Data	NASA	$323,033	1 Jul 1994- 30 Jun 1997	17

...end...

Plate 1.

Fraction of a field of view which is covered by rain. The red curve is used for the 37 GHz channels, the green curve for the others. These relations are adapted from the results of C.E. Graves, J. Atmos. and Ocean. Tech., Vol 10 (1993), p. 5-14, Tables 1 & 2.

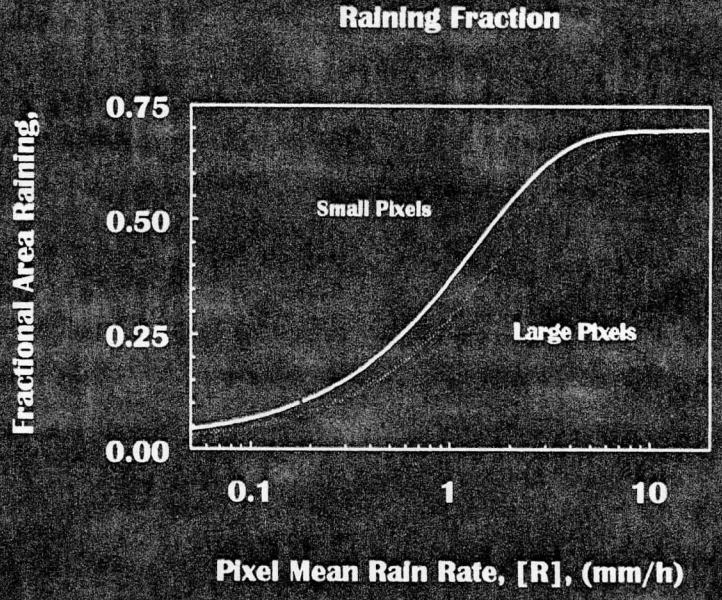

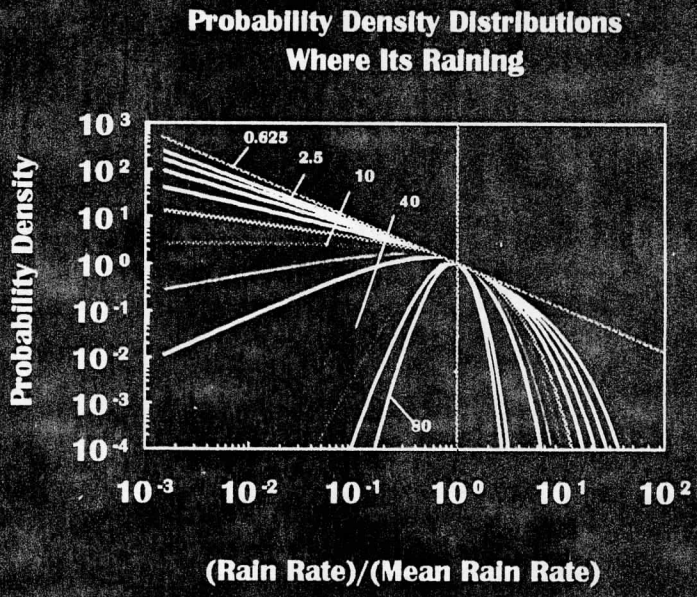

Adopted probability density distributions for various values of mean rain rate (where raining). The curves are normalized to 1 where $R/R_{mean}=1$. Labels indicate the mean rain rate. Note that the X-axis is also scaled by the mean rain rate where raining.

Plate 2.

SMMR channel rain rates as functions of brightness temperature when environmental conditions are fixed at nominal values:

Relative hum. 80%, sea sfce. temp. 27.15°C, wind 7 m/s, freezing level 4.5 km.

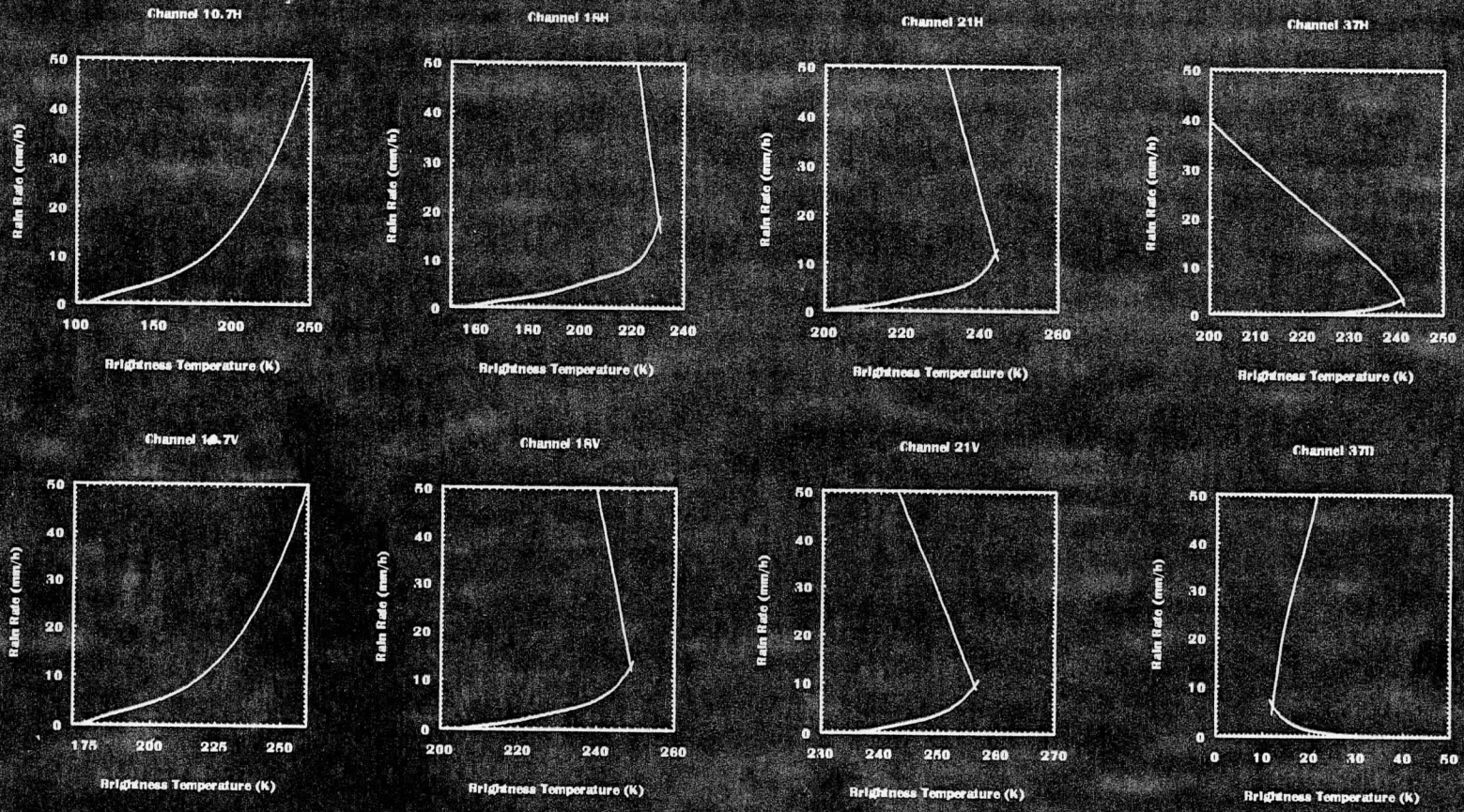

Plate 3.

Changes in SMMR channel rain rates as functions of brightness temperature when environmental conditions vary around the fixed at nominal values:

Relative hum. 80%, sea sfce. temp. 27.15°C, wind 7 m/s, freezing level 4.5 km.

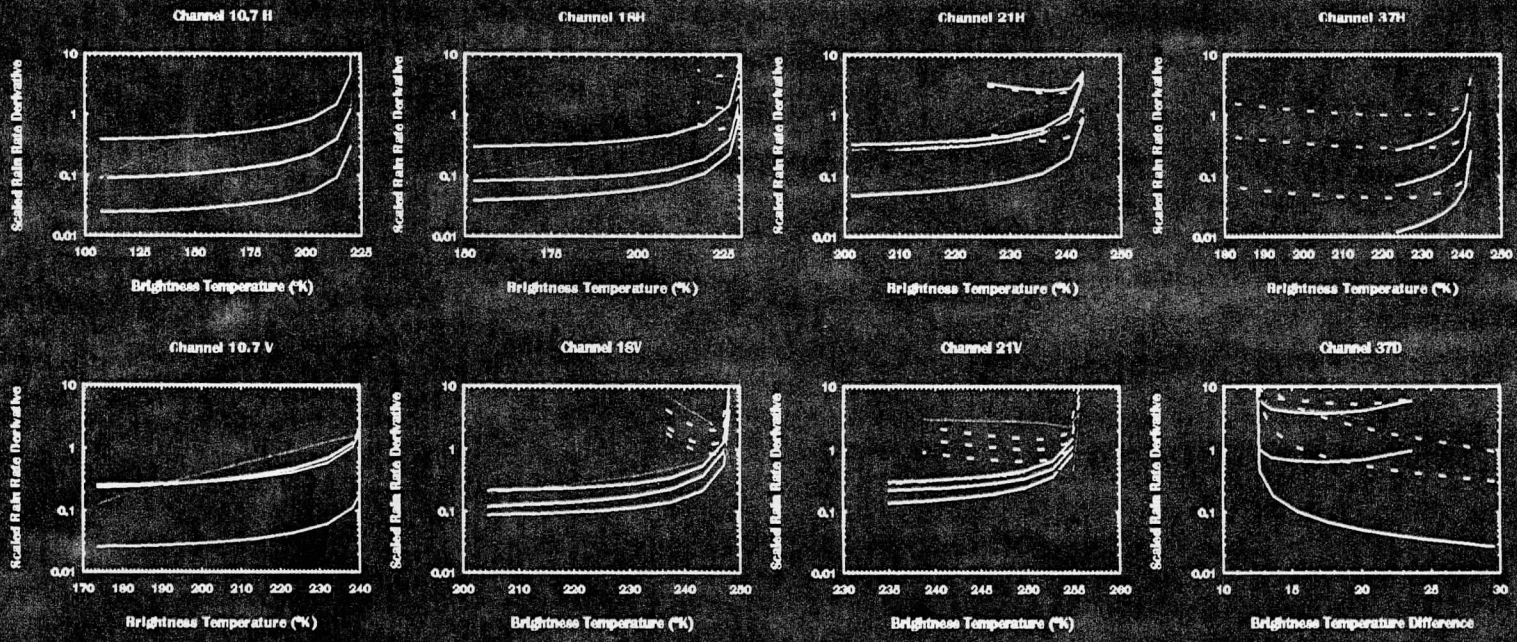

Scaled derivatives are partials with respect to one of the parameters times a typical variation in that parameter –3 degrees for SST (yellow), 5% for relative humidity (orange), ½ km for freezing level (lt. blue), and 3 m/s for wind (magenta). Negative values are shown dashed.

Plate 4

Sensitivity of Weights to Error Components

Normal Weights

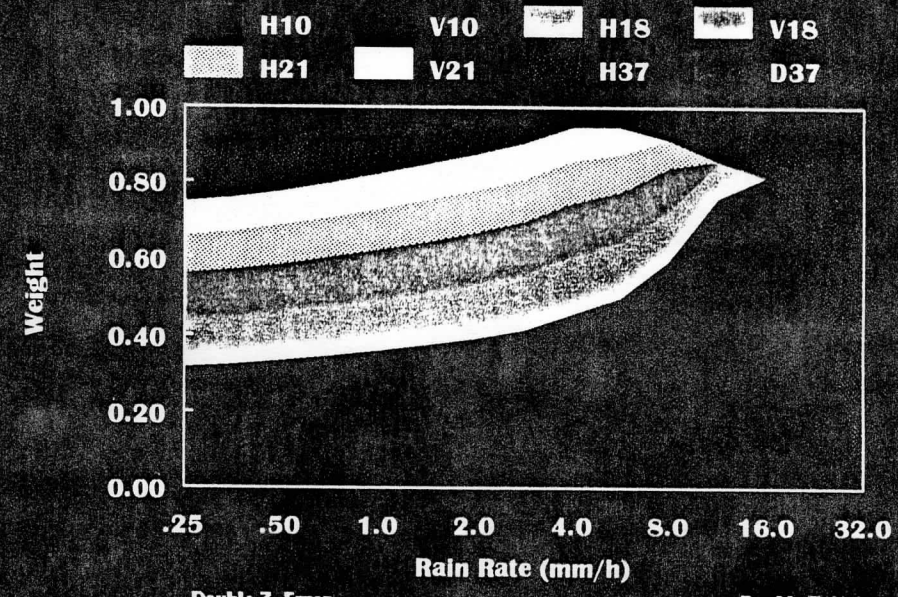

Double Wind Error

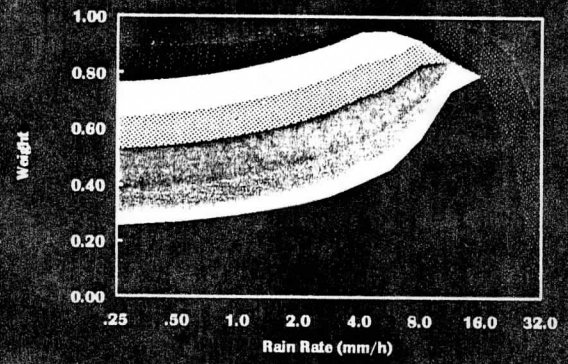

Double SST Error

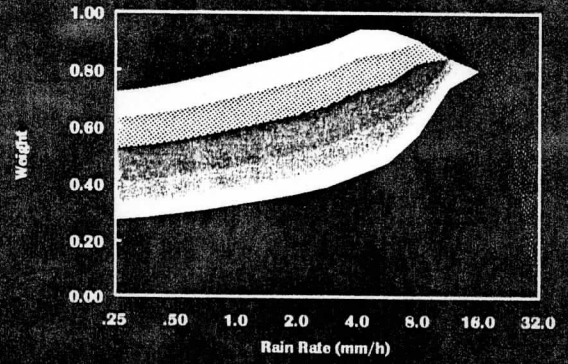

Double RH Error

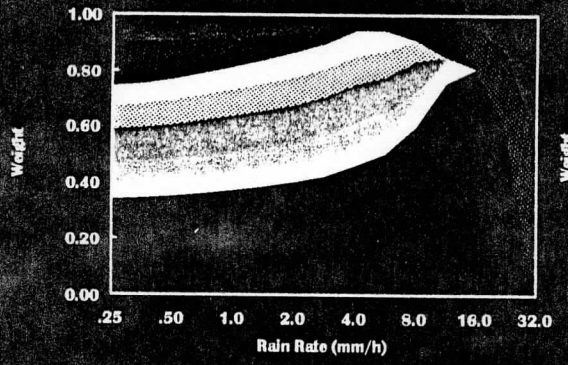

Double Z_T Error

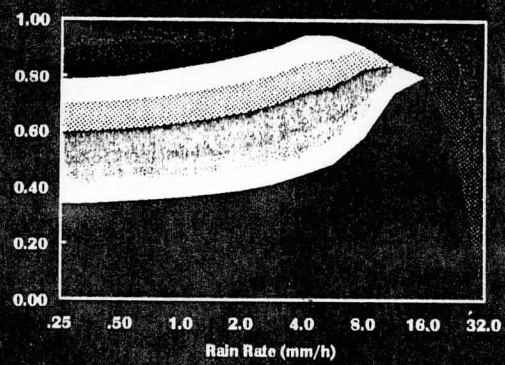

Double T_B Noise